

# Electron field emission from diamond-like carbon, a correlation with surface modifications

Peter Grant and Christophe Py<sup>a)</sup>

*Institute for Microstructural Sciences, National Research Council of Canada, Montreal Road, Ottawa Ontario KIAOR6, Canada*

Claudia Mößner

*SI Software Innovation, 67346 Neustadt, Germany*

Alexandre Blais

*Département de Physique et Centre de Recherche en Physique du Solide, Université de Sherbrooke, Sherbrooke, Québec J1K 2R1, Canada*

Hue Tran and Mae Gao

*Institute for Microstructural Sciences, National Research Council of Canada, Montreal Road, Ottawa Ontario KIAOR6, Canada*

(Received 14 July 1999; accepted for publication 25 October 1999)

We report a series of experiments characterizing the emission obtained from near-amorphous carbon deposited by excimer laser ablation. We found that vacuum arc discharge and material transfer are responsible for morphology modifications that greatly enhance emission. When the morphology of the materials are well controlled, we find that our carbon has a work function one half that of silicon. [S0021-8979(00)06803-1]

## INTRODUCTION

Great effort has been invested in the past years for the development of reliable field emitters for field emission displays (FED). Several approaches have been investigated, the most common being the Spindt type emitters.<sup>1</sup> It has been shown that impressive and stable current could be drawn from an array of these tips. However, their fabrication into arrays, which are necessary for commercialization, is still a technical challenge. More recently, a lot of interest has been focused on diamond-like carbon (DLC) because of its FED compatible chemical and physical properties. DLC films were reported to emit at relatively low fields, as low as a few tens of V/ $\mu\text{m}$ .<sup>2,3</sup> Hence, DLC could resolve the necessity for arrays of tips as was shown by SIDT.<sup>4</sup> It could also be applied as a coating for arrays of Spindt-type tips providing protection against deterioration in a static vacuum, and possibly enhance emission.<sup>5,6</sup> However, the mechanism of emission was not well understood and very low values of work function were erroneously attributed to DLC. Several approaches have been developed to explain low field emission: negative electron affinity (NEA), and emission from impurities, among others. It was pointed out by Gröning *et al.*<sup>7</sup> and Talin *et al.*<sup>8</sup> that the high currents at low field often seen in the literature could be due to enhancement of the field magnification factor,  $\beta$ , due to localized surface modifications. They reported formation of craters in the diamond film due to field emission (FE) initiated discharges. This article supports those observations and demonstrates that other types of surface modification occur during FE.

## EXPERIMENTAL SETUP

The DLC films used in these experiments were deposited using excimer pulsed laser deposition (PLD). High purity graphite targets were used and the films were deposited on silicon substrates. In this article we refer to our films as DLC, but amorphous carbon may be a more accurate description. The films are very smooth, hard, and free of grain structure visible by scanning electron microscopy (SEM) or optical means. The bonding is mainly  $sp^2$  with some  $sp^3$  as determined by Raman spectrometry. A detailed description of those films has been made elsewhere.<sup>9</sup> All field emission measurements were conducted in a turbo pumped vacuum chamber at pressure less than  $4 \times 10^{-6}$  Torr.

To form a reference, measurements were also conducted on  $n$ -type, low resistivity, 0.01–0.02  $\Omega$  cm, silicon wafers. The substrates carrying the carbon films were cleaved in 1 cm squares that were then washed in ethyl alcohol and water with ultrasonics for 10 min. They were then washed for 10 more minutes in ethyl alcohol with ultrasonics. Finally, they were blown dry with ultrahigh purity nitrogen. In order to avoid surface contamination, the silicon wafers were cleaved in a clean room environment and only exposed to ambient atmosphere just before measurement.

A simple test cell made with a DLC film, a conducting anode and two glass spacers was constructed for measuring the surface emission. Glass spacers of various thickness could be used to adjust the spacing between the cathode and anode. The cathode and anode were offset so that leads could be conveniently connected away from the area of high electric field, which was typically 5 mm $\times$ 5 mm. A drawing showing test cell construction is shown in Fig. 1. The cathode was usually a DLC coating on a silicon substrate. The anode was stainless steel or sometimes a ZnO phosphor

<sup>a)</sup>Electronic mail: christophe.py@nrc.ca

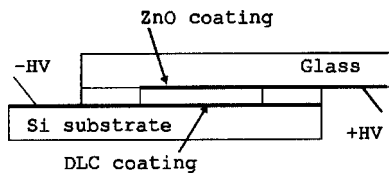


FIG. 1. Schematic of test cell used to observe emission spots.

coated piece of glass. A computer controlled data acquisition system was used to increase the voltage applied to the cell while recording current. It was observed that sequential application of voltage usually produced successively higher emission current. In fact, there was often no emission current up to the maximum voltage applied to these cells of 5 kV which with a spacer height of 200  $\mu\text{m}$  gave a field of 250 kV/cm. Subsequent application of voltage to a nonemitting film could give a current. When the ZnO coated glass was used as the anode light could be observed coming from the cell, but only from discrete areas. No large area emission was observed with this setup. Only a small number of bright dots were visible. The emitting areas could not be measured precisely, but were approximately the same dimension as the thickness of the spacer, i.e., the same as the anode to cathode gap. In one observation, a thin film that appeared to emit well based on a current versus voltage measurement was observed to emit from a single point.

To permit examining a restricted area of the film a second test cell was constructed as shown in Fig. 2. The anode was either a Pt-Ir scanning tunneling microscope tip or a 1 mm diameter copper cylinder. The cathode-anode gap was adjusted with a micrometer under an optical microscope. This distance was set to 75  $\mu\text{m}$  with an error evaluated to be approximately 10  $\mu\text{m}$ . With the Pt-Ir anode, the area of the sample that was subjected to high electric field was a circle, about 100  $\mu\text{m}$  in diameter. Negative voltage was applied to the coated side of the sample. While measuring current, the electric field was increased to 1300 kV/cm and was then brought back to 0 kV/cm in order to show the hysteresis in the current-voltage ( $I$ - $V$ ) characteristic.

### VACUUM ARC DISCHARGE, MATERIAL TRANSFER, AND SURFACE MODIFICATIONS

The surface of the carbon films was investigated before measurement using an 800X optical microscope equipped with a charge-coupled device (CCD) camera. A circle of 1

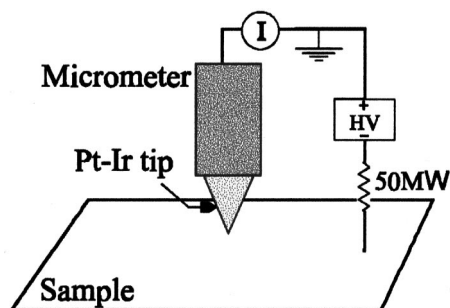


FIG. 2. Schematic of measuring apparatus showing the Pt-Ir anode.

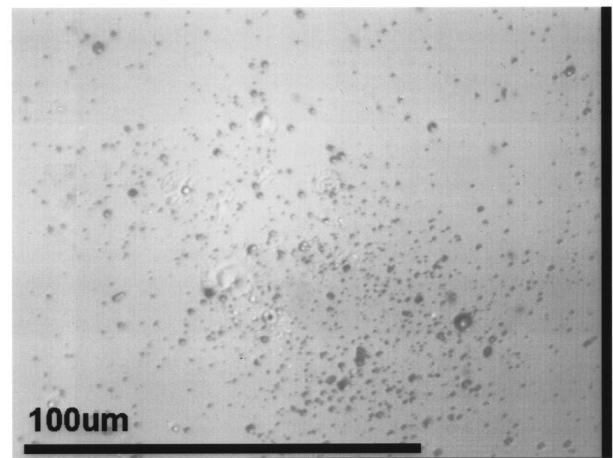


FIG. 3. Optical micrograph of a silicon wafer showing craters formed by anode material impact.

mm in diameter was used to identify the cleanest areas. Hence, the surface of the films was well characterized prior to FE measurements. The surface of the samples was examined after measurement using the 800X optical microscope; they were also characterized with SEM, atomic force microscopy (AFM), and energy dispersive x-ray (EDX) analysis. The integrity of the silicon wafers was verified using these techniques to probe outside the region of interaction with the high electric field and all analysis revealed clean and regular surfaces. No FE from PLD carbon films was measured to fields up to 1300 kV/cm. In some cases, emission was measured at fields as low as 300 kV/cm, but a careful examination of the sample showed that surface modification had occurred during FE measurement. Similar surface modification was also observed for uncoated silicon wafers. An optical micrograph, Fig. 3, of a silicon wafer, on which FE measurement was conducted, shows a crater formation. This crater is apparently due to the impact of anode material. In this case, the copper anode was used and an EDX analysis confirmed the presence of copper on the cathode. The quantity of copper was small. An EDX survey did not detect copper above the background. It was necessary to examine the SEM image and investigate any features that seemed to be anomalous in either shape or brightness. One piece of copper metal was discovered in this way. Material transfer probably occurred during a vacuum arc discharge (VAD) which occurred between the silicon wafer and the copper cylinder. However, the process of a VAD is not yet completely understood. A discharge could occur when protrusions or impurities on the cathode start emitting electrons following the Fowler-Nordheim (F-N) relation. This emission would cause heating of the anode and cathode protrusions, where the current density is the greatest, through resistive heating which would then evaporate enough material for a spark to occur.<sup>10</sup> Emitted electrons could also ionize residual gases or evaporated material, which in turn would cause sputtering of the cathode releasing more material and leading to a discharge. On the particular sample shown on Fig. 3, the current increased by several orders of magnitude after the VAD, Fig. 4. This  $I$ - $V$  curve shows the same hysteresis characteristic described by

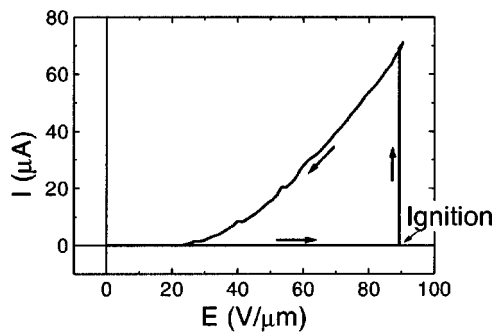


FIG. 4. No emission was measured until an ignition occurred. Electron emission increased several orders of magnitude after the vacuum arc discharge.

Gröening *et al.*,<sup>11</sup> but in this case it is produced by transferred material from anode to cathode forming a crater instead of a vacuum arc discharge evaporating cathode material and resulting in a crater.

Formation of craters is not required to obtain an  $I$ - $V$  characteristic with hysteresis. Transfer of anode material, without formation of craters, proved to be sufficient in order to obtain enhanced emission. Such surface modifications can create high  $\beta$  protrusions that could explain the high level of current observed. Hence, a careful examination of the film surface before and after FE measurement is important in order to deduce physically meaningful film properties from a F-N plot.

Anode material and geometry are important parameters to control in order to avoid material transfer. Materials with high boiling points have proved to be more appropriate, hence Pt-Ir is more suitable than copper for this purpose. The shape of the anode is also an important parameter. A needle shaped anode, with a high radius of curvature, will sustain a high current density and will experience a rapid temperature rise through resistive heating. High anode temperature, as pointed out previously, will cause gas to be released, eventually leading to a VAD. For this reason, an anode having a large area would be preferable. Nevertheless, protrusions, even on a large anode, will sustain high current densities. Formation of such protrusions on the anode is to be expected to occur during field emission. In order to clearly demonstrate this effect, a silicon wafer was used and the polarity was reversed, i.e., the silicon was made the anode and the Pt-Ir tip the cathode. Figure 5 is a 800X optical micrograph showing the resultant surface morphology changes. With a maximum current of  $30 \mu\text{A}$ , corresponding to a power density of  $1910 \text{ W/cm}^2$ , temperatures sufficient to melt the silicon anode were reached. A  $100 \mu\text{m}$  diameter ring, which is likely due to heating, can also be seen around the melted area. The diameter of this ring is near the size of the cathode-anode gap. Hence, damage occurs on the anode during field emission due to the power delivered by the high energy electrons.

We note that we have attempted to use AFM to measure  $\beta$  directly. Figure 6 is an AFM image of a  $4 \mu\text{m} \times 4 \mu\text{m}$  area of a typical DLC surface. What we find on clean DLC is that most of the surface is smooth, has bumps of about 2 nm height, and 20 nm horizontal extent. There are numerous

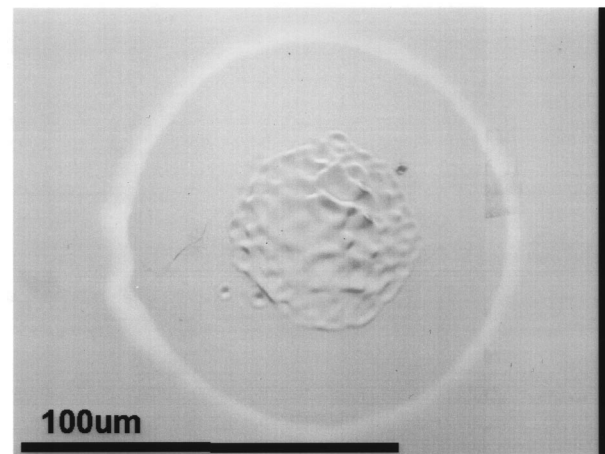


FIG. 5. An optical micrograph (800 $\times$ ) showing a melted area on a Si anode. A  $\approx 100 \mu\text{m}$  ring can be seen around the melted area.

higher features, having heights of 20 nm that appear as light dots in Fig. 6. A number of dots were examined using the computer software in the AFM. It was found that the horizontal extent of the white dots was about  $10\times$  more than their height. That is, we found no evidence for a large field magnification factor on clean DLC films. After activation this is not the case. The films were covered with features that appeared as abrupt walls that could not be imaged by AFM. That is because the AFM tip was formed from a cone with an angle of 57 deg. We can only observe surface features that form a smaller angle than 57 deg from the sample normal. Thus, we conclude that AFM is not a suitable tool for searching for small radius features on top of high points on the film.

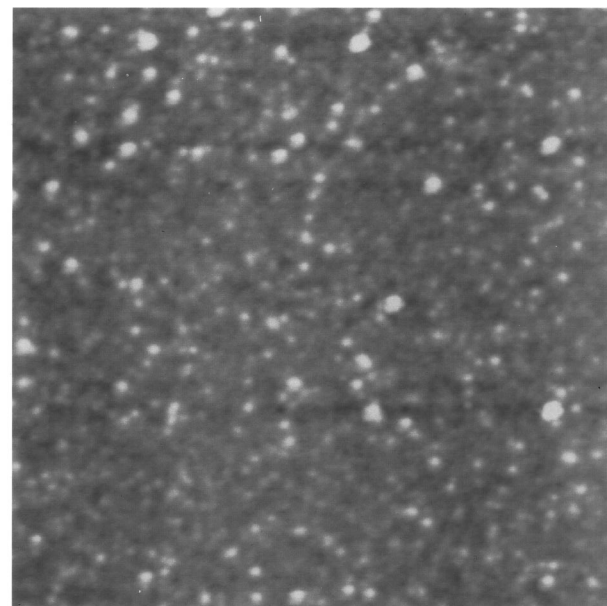


FIG. 6. Atomic force microscope image of a pulse laser deposited diamond-like carbon film shows a smooth surface with some high features.

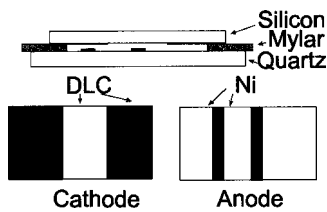


FIG. 7. Schematic of a cell used to compare emission from bare silicon with that of diamond-like carbon coated silicon.

**COMPARISON OF THE WORK FUNCTIONS OF CARBON AND SILICON**

An attempt was made to produce an activation of bare silicon using the needle as anode. Because of the large gap of  $75 \mu\text{m}$ , we were able to only generate fields of  $1300 \text{ kV/cm}$ . When emission was found from silicon, a surface examination by optical microscope revealed that extensive surface modifications had taken place. We believe that such surface modifications will be difficult to eliminate when using high voltages and large gaps. That is because the capacitance of the test cell and wiring store energy proportional to voltage squared. When a VAD occurs, a very fast, high power density discharge occurs in the small sample volume. A  $50 \text{ M}\Omega$  resistor was included in series with the high voltage lead to reduce the power delivered by the cable capacitance during a VAD. However, it does not eliminate the energy stored in the cell itself. Two lower voltage experiments were also conducted.

Figure 7 is a schematic of cell that was used to compare emission from bare silicon with that of DLC coated silicon. For this cell, the vacuum system was baked for 48 h before bias voltages were applied. The cathode is a silicon wafer that was coated using a shadow mask to keep one half of the area free of DLC. The anode was made of nickel deposited on a quartz substrate by electron beam evaporation. As with the cathode, a shadow mask was used to define two stripes. The two substrates were separated by  $12 \mu\text{m}$  mylar shims at the periphery of the test cell. The mylar was far from the region where the electric field was generated; the quartz substrate provided the electrical insulation. During testing, only one anode was connected at a time. First the DLC anode was grounded and emission was measured. Then the DLC coated cathode was allowed to float and the bare silicon cathode was measured. During the measurement of the silicon anode, emission from the DLC side was allowed to bias the anode

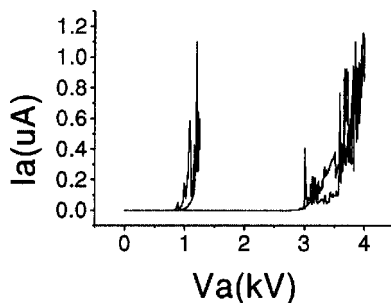


FIG. 8. Fowler-Nordheim plot showing the side-by-side test of flat silicon and diamond-like carbon surfaces.

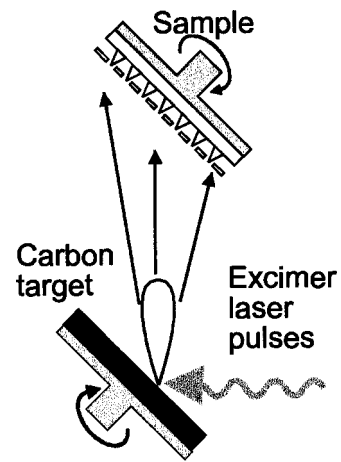


FIG. 9. Laser ablation deposition method for carbon on a rotated, tilted sample.

facing the DLC to a high voltage. This was done to prevent damage to the DLC side of the cell during testing at the higher voltages needed to achieve emission from the silicon side of the cell. The system had been previously tested at the highest voltages to be used to confirm that there was no leakage current from any of the connections.

The results are shown in Fig. 8. With a fresh anode, cathode, and a vacuum system as clean as we could make it, it was found that there was a consistent ratio between emission from silicon and DLC coated silicon. The samples were subjected to a series of voltage scans. Voltage was increased until some particular current level was reached and then voltage was reduced to zero. On both bare silicon and DLC coated silicon it was found that the more a sample was scanned the lower the threshold of emission became. This we attribute to surface roughening under bias. While the absolute voltage was found to decrease with time under bias, the ratio of voltages remained consistent at about  $3\times$  higher for bare silicon. Assuming that the roughness of silicon and DLC films were the same, we found that our carbon films had a work function twice as low as silicon.

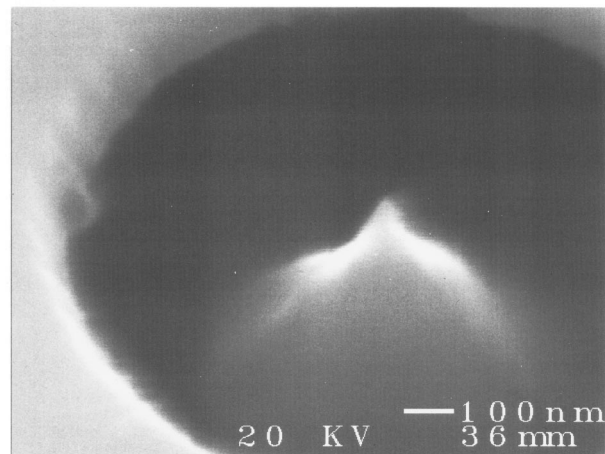


FIG. 10. Scanning electron microscope image of a microtip coated with 20 nm of carbon.

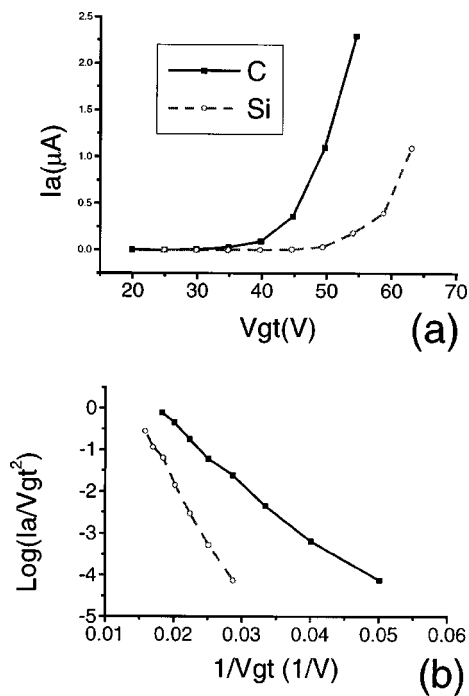


FIG. 11. (a) Emitted current as a function of gate voltage and (b) Fowler–Nordheim plot of silicon microtips before and after coating with carbon.

However, as has been pointed out, surface morphology is paramount in the occurrence of FE so this ratio had to be confirmed in an experiment where the electric field was as independent of surface morphology as possible. Gated silicon microtips were coated with DLC. The construction process for these tips is described elsewhere.<sup>12</sup> In these microtips the spacing from cathode to gate is approximately  $0.65 \mu\text{m}$ . The DLC films were deposited using laser ablation by mounting the cathode on a rotating stage such that the incident vapor arrived at the tip approximately normal to the surface. A schematic diagram of the coating method is shown in Fig. 9. Initial coatings were performed without tilting the cathode, however this seemed to result in no carbon coatings on the tips of the emitters. The explanation for this is that near the tip of the emitter the surface is almost parallel to the incident vapor resulting in a very thin film. The DLC film thickness was restricted to 20 nm to limit the extent to which the film thickness would perturb the electric field in the emitter.

Figure 10 is an SEM micrograph of a DLC coated tip. There is no evidence in the SEM image of the carbon coating, or of its thickness. The thickness was deduced from a witness sample during coating. The  $I$ – $V$  and  $F$ – $N$  plots of the cathode before and after coating are shown in Fig. 11. The slope of the curves gives the combination of field magnification factor and work function. The ratio of the slopes is

approximately 2. That is, the work function of silicon is about 2 times that of DLC.

## DISCUSSION OF LOW FIELD EMISSION

We find field emission at anomalously low electric fields from surfaces other than DLC, particularly silicon that has been subjected to high electric fields. Surfaces that were initially coated with DLC are always better emitters than surfaces that were initially bare silicon. After field emission has been observed, the surfaces are rough, sometimes include material deposited from the anode, and are sufficiently complex that we cannot say precisely where or what is responsible for the emission.

We draw three conclusions from this study:

(1) We have never observed field emission at anomalously low electric fields from clean smooth well characterized thin films.

(2) By using microtips coated with DLC, we find that the work function of excimer laser ablation deposited DLC to be about 0.5 that of silicon.

(3) While we cannot rule out the possibility of low work function material being produced at particle or grain boundaries, our observations indicate that surface roughness is a suitable explanation for electron emission at low electric fields from DLC.

The work function of the silicon cathodes used as a reference is about 4.3. This means that our carbon has a work function of about 2.15. While this value is not as low as some other studies have found, it still justifies interest in this material for FEDs. We believe that it is best used as a thin coating on top of gated microtips.

<sup>1</sup>C. A. Spindt, I. Brodie, L. Humphrey, and E. R. Westerberg, *J. Appl. Phys.* **47**, 5248 (1976).

<sup>2</sup>F. Y. Chuang, C. Y. Sun, T. T. Chen, and I. N. Lin, *Appl. Phys. Lett.* **69**, 3504 (1996).

<sup>3</sup>Z. Feng, I. G. Brown, and J. W. Ager III, *J. Mater. Res.* **10**, 1585 (1995).

<sup>4</sup>H. Kumar, H. K. Schmidt, M. H. Clark, A. Ross, B. Lin, L. Fredin, B. Baker, D. Patterson, and W. Brookover, *SID Digest* **25**, 43 (1994).

<sup>5</sup>J. A. Dobrowolski, P. D. Grant, P. Laou, L. Li, C. Moessner, L. M. Plante, C. Py, C. X. Qiu, I. Shih, R. H. Simpson, B. T. Sullivan, H. T. Tran, and A. J. Waldorf, *Physics in Canada* **52**(5), 207 (1996).

<sup>6</sup>S. Lee, J. H. Jung, B. K. Ju, Y. H. Lee, M. H. Oh, and D. Jeon, *SID Digest* **28**, 603 (1997).

<sup>7</sup>O. Gröning, O. M. Küttel, E. Schaller, P. Gröning, and L. Sclapbach, *Appl. Phys. Lett.* **69**, 476 (1996).

<sup>8</sup>A. A. Talin, F. E. Felter, M. P. Siegal, T. A. Friedmann, J. P. Sullivan, and M. P. Siegal, *J. Vac. Sci. Technol. A* **14**, 1719 (1996).

<sup>9</sup>C. Moessner, P. Grant, H. Tran, G. Clarke, D. J. Lockwood, H. J. Labbé, B. Mason, and I. Sproule, *Mater. Res. Soc. Symp. Proc.* **423**, 699 (1996).

<sup>10</sup>J. M. Meek and J. D. Craggs, *Electrical Breakdown of Gases* (Wiley, New York, 1978), pp. 129–208.

<sup>11</sup>V. Nutzandel, O. M. Küttel, O. Gröning, and L. Sclapbach, *Appl. Phys. Lett.* **69**, 2662 (1996).

<sup>12</sup>C. Py, M. Gao, and P. D. Grant, *Physics in Canada*, **54**(4), 217 (1998).